Inorganic Chemistry

Article

pubs.acs.org/IC

Acid/Base-Controlled Au^I/Au^0 Reductive Transformations of the Monogold $[(\mu_{14}\text{-Au})Pd_{22}(CO)_{20}(PEt_3)_8]^+$ Monocation into Three Different Neutral Digold Nanoclusters: $Au_2Pd_{21}(CO)_{20}(PEt_3)_{10}$, $Au_2Pd_{28}(CO)_{26}(PEt_3)_{10}$, and New Five-Layer Hexagonal Close-Packed $(\mu_{12}\text{-Au})_2Pd_{42}(CO)_{30}(PEt_3)_{12}$ with a Trigonal-Bipyramidal $AuPd_3Au$ Kernel

Evgueni G. Mednikov* and Lawrence F. Dahl*

Department of Chemistry, University of Wisconsin—Madison, Madison, Wisconsin 53706, United States

Supporting Information

ABSTRACT: The *monogold* $[(\mu_{14}\text{-Au})Pd_{22}(CO)_{20}(PEt_3)_8]^+$ nanocation (**2**, with a $[(CF_3CO_2)_2H]^-$ counterion) is shown to be a versatile precursor for the generation of three different neutral Au−Pd nanoclusters with *double* gold content in their distinctly dissimilar bimetallic architectures. These carbon monoxide (CO)-induced conversions are based on the reduction of Au^I to Au^0 that is controlled by the reaction medium. Under basic and acidic conditions, the known $Au_2Pd_{21}(CO)_{20}(PEt_3)_{10}$ (**3**; >90% yield) and $Au_2Pd_{28}(CO)_{26}(PEt_3)_{10}$ (**4**; ∼40% yield), respectively, were obtained, whereas neutral conditions gave rise to the new $(\mu_{12}\text{-Au})_2Pd_{42}(CO)_{30}(PEt_3)_{12}$ (**1**; ∼10−20% yield; all yields based on gold). The molecular structure of **1**, established from a 100 K CCD X-ray diffraction study, consists of a *five-layer* hexoganol close-packed (hcp) Au_2Pd_{42} framework of *pseudo*-D_{3h} symmetry (crystallographic D_3 site symmetry) of the $Pd_6/AuPd_9/Pd_{12}/AuPd_9/Pd_6$ layer sequence, with the Au atoms centering two identical hcp $(\mu_{12}\text{-Au})Pd_{12}$ *face-fused anti*-cuboctahedral fragments. The 12 Et_3-attached P atoms are coordinated to the triangular vertex Pd atoms in the four outer layers (except the middle Pd_{12}); all five layers are stapled by *interlayer* bridging COs. The radial Au_{cent}−Pd mean distance of 2.79 Å within the two symmetry-equivalent $(\mu_{12}\text{-Au})Pd_{12}$ *anti*-cuboctahedral fragments of **1** is identical with the radial Pd_{cent}−Pd mean distances within hcp $(\mu_{12}\text{-Pd})Pd_{12}$ *anti*-cuboctahedral fragments of the two geometrically related nondistorted layered structures of $Pd_{52}(CO)_{36}(PEt_3)_{14}$ and $[Ni_9Pd_{33}(CO)_{41}(PPh_3)_6]^{4-}$ ($[PPh_4]^+$ counterion), indicating a strain-free structural effect upon the substitution of Au for Pd in their analogous hcp layer-stacked arrangements. It provides prime evidence for an extension to **1** of our previous self-consistent experimental/theoretical-based hypothesis for delocalization of the 6s valence Au electrons in Au_2Pd_{21} (**3**) and Au_2Pd_{28} (**4**) toward a formal closed-shell Au^+ configuration that is electronically equivalent to that of zerovalent Pd.

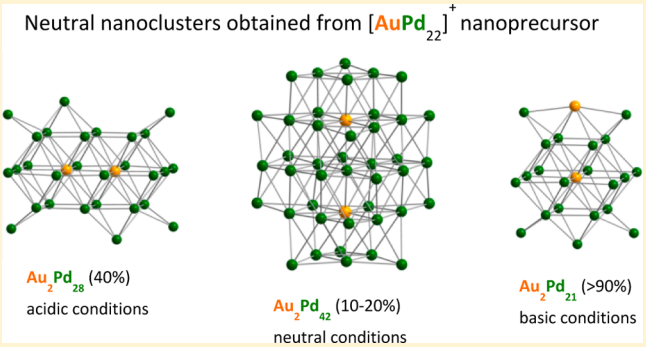

INTRODUCTION

Reductive condensation is a prime way to generate transition-metal carbonyl clusters from commonly available metal salts as well as from preformed metal carbonyls.[1] Most of the resultant clusters are without interstitial metal atoms and normally contain less than 8−12 metal atoms. Conditions for their further conversions into nanosized clusters are generally not obvious.[2] However, whenever appropriate nanoprecursors become available, they are used for further transformations,[3] giving rise (sometimes with high selectivities) to other nanosized clusters that, at least for palladium, are unlikely to be obtained by the reduction of conventional palladium(II) salts.[4]

Herein we report reactions of the $[(\mu_{14}\text{-Au})Pd_{22}(CO)_{20}(PEt_3)_8]^+$ monocation (**2**, as the $[(CF_3CO_2)_2H]^-$ salt)[5a] under different conditions that give rise to three neutral Au−Pd nanoclusters including one with a new stacked five-layer hexoganol close-packed (hcp) Au_2Pd_{42} geometry of *pseudo*-D_{3h} symmetry, which is reduced to crystallographic D_3 site symmetry upon inclusion of its carbonyl ligands. These syntheses illustrate an important breakthrough in the formation of nanosized heterometallic Au−Pd clusters by utilization of a readily available Au−Pd nanoprecursor. Our research also provides insight concerning the important roles that palladium-by-gold substitution and carbon monoxide (CO) play in

Special Issue: To Honor the Memory of Prof. John D. Corbett

Received: October 13, 2014
Published: November 26, 2014

dx.doi.org/10.1021/ic502470m | Inorg. Chem. 2015, 54, 1145−1151

mediating the formation and properties of nanosized palladium clusters. In demonstrating experimentally the CO stability of zerovalent Au^0–Pd nanoclusters relative to that of CO-unstable homopalladium ones[3e,5a] [in accordance with density functional theory (DFT) calculations], it has direct relevance to recent reports of bimetallic Au–Pd nanoparticle catalysts that have much greater activities[6a−c] and stabilities[6d] and higher tolerance to CO poisoning than monometallic palladium counterparts.[6e]

RESULTS AND DISCUSSION

The three *digold* nanoclusters generated from the medium-controlled *reductive* conversions of the *monogold* monocation **2**[5a] are the known $Au_2Pd_{21}(CO)_{20}(PEt_3)_{10}$ (**3**)[5b] and $Au_2Pd_{28}(CO)_{26}(PEt_3)_{10}$ (**4**)[3e] and the new nanosized $(\mu_{12}\text{-}Au)_2Pd_{42}(CO)_{30}(PEt_3)_{12}$ (**1**). These transformations result in the doubling of the gold content in the clusters.

In a *basic medium* [in Me_2CO/tetrahydrofuran (THF) under CO or in *N*,*N*-dimethylformamide (DMF) under N_2]:

$$2[AuPd_{22}(CO)_{20}(PEt_3)_8][(CF_3CO_2)_2H] + CO + 4NH_4OH \xrightarrow[\text{-'PEt}_3\text{', -'Pd', -'extra CO'}]{} \underset{\mathbf{3}}{Au_2Pd_{21}(CO)_{20}(PEt_3)_{10}} + CO_2 + 4[NH_4][CF_3CO_2] + 3H_2O \quad (1)$$

In a *neutral or acidic medium* (in MeCN or in Me_2CO/CF_3CO_2H):

$$2[AuPd_{22}(CO)_{20}(PEt_3)_8][(CF_3CO_2)_2H] + CO + H_2O \xrightarrow[\text{-'PEt}_3\text{', -'Pd', -'extra CO'}]{} \underset{\mathbf{1}}{Au_2Pd_{42}(CO)_{30}(PEt_3)_{12}}$$
$$\text{or } \underset{\mathbf{4}}{Au_2Pd_{28}(CO)_{26}(PEt_3)_{10}} + CO_2 + 4CF_3CO_2H \quad (2)$$

Reaction (1) under basic conditions is greatly favored because of (a) the much higher nucleophilic character of OH^- compared to that of the water molecule and (b) the formation of water. This reaction gives a virtually quantitative yield of **3** (>90%). The formation of **4** in reaction (2) under acidic conditions occurs readily (~40%); however, the preparation of **1** under neutral conditions (10–20% yield; all yields based on gold) requires a preliminary treatment of dried precursor **2** with CO prior to CH_3CN extraction under N_2. In reactions (1) and (2), the release of excessive palladium and ligands occurs due to the formation of unidentified $Pd_n(CO)_x(PEt_3)_y$ clusters with variable stoichiometries,[2b,7] as well as CO(g) and $[HPEt_3]$-$[CF_3CO_2]$ salt (under acidic conditions).

The known nanoprecursor **2** (Figure 1), obtained in 45–60% yield from two-step/one-pot reactions of $Pd_{10}(CO)_{12}(PEt_3)_6$ with CF_3CO_2H and $Me_3NO{\cdot}2H_2O$ (in acetone at 50 °C), followed by ion exchange of proton(s) with Au^+ [from $Au(SMe_2)Cl$],[5a] represents the only isolated Au–Pd carbonyl nanocluster with the Au atom in a formal Au^I oxidation state.[8] The capability of **2** for facile reduction arises from its nature. Indeed, it contains both the reductant, CO, and oxidant, Au^I. Its positive charge delocalized over the metal cluster surface facilitates the nucleophilic attack of OH^- anions to oxidize CO into CO_2 with the concomitant reduction of Au^I into Au^0; the resulting generation and condensation of the presumably neutral coordinatively unsaturated CO/PEt_3-ligated $AuPd_n$ species give rise to the digold **3**. Under basic conditions, the Au_2Pd_{21} **3** can also be obtained from **2** under N_2 (instead of a CO atmosphere). On the other hand, we have never observed the formation of either **1** or **4** in the absence of CO. Thus, under acidic and neutral conditions (in the presence of the weak H_2O nucleophile instead of OH^-), the *initial* step presumably involves fragmentation of precursor **2** under a CO atmosphere.

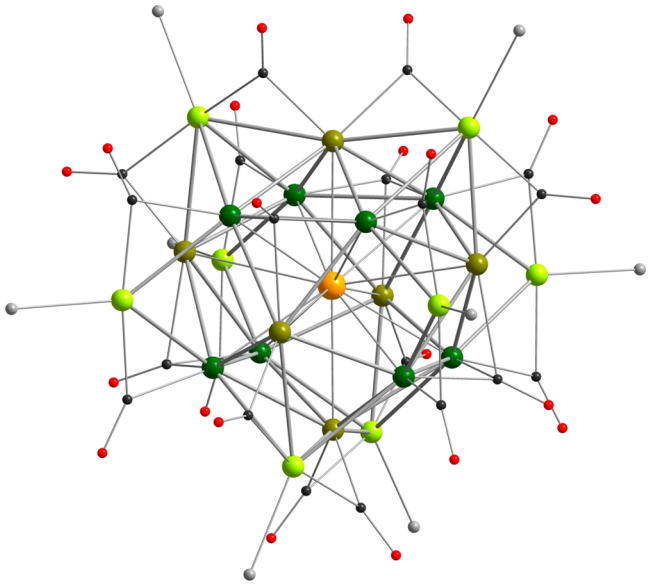

Figure 1. *Pseudo-*D_{2d} ($\bar{4}2m$) geometry (without P-attached Et substituents) of the monocationic nanoprecursor **2** (isostructural as both $[(CF_3CO_2)_2H]^-$ and $[PF_6]^-$ salts).[5a] The central encapsulated Au^I (yellow) is connected to 14 Pd atoms in the $(\mu_{14}\text{-}Au)Pd_{14}$ kernel composed of 8 Pd atoms (dark green) in a highly deformed Pd_8 cube and 6 Pd atoms (olive green) that cap all six cubic Pd_4 faces. This $AuPd_{14}$ kernel is augmented by eight additional PEt_3-ligated Pd atoms (light green) comprised of four dicapped and four tetracapped Pd atoms. The 20 bridging carbonyl ligands consist of 16 doubly bridging COs (with two COs coordinated to each of the eight PEt_3-ligated Pd atoms) and four triply bridging COs (each connected to two Pd atoms linked by one of the four electron-pair Pd–Pd bonds in the top/bottom Pd_4 cubic faces and to one Pd atom of the four horizontal face-capped Pd atoms).

In our previous study,[3e] the CO-stable Au_2Pd_{28} **4** was obtained in 25–30% yield from the *nonredox* condensation of CO-stable Au_2Pd_{21} **3** with coordinatively unsaturated homopalladium species resulting from CO-induced fragmentations under CO of the CO-unstable (but structurally similar) $Pd_{23}(CO)_{20}(PEt_3)_{10}$; our hypothesis that its synthesis is initially induced by the CO atmosphere was then substantiated by obtaining Au_2Pd_{28} **4** with similar 25% yield from an analogous reaction involving substitution of the homopalladium Pd_{23} coreactant with the structurally dissimilar but also CO-unstable $Pd_{38}(CO)_{28}(PEt_3)_{12}$. In contrast to CO-stable Au_2Pd_{21}, the monocation **2** possesses moderate reactivity toward CO.[9] Hence, reaction (2) that produces Au_2Pd_{28} **4** from the $AuPd_{22}$ monocation under acidic conditions mimics the previous procedure,[3e] which necessitated the use of the CO-unstable homopalladium Pd_{23} or Pd_{38} coreactant to furnish coordinatively unsaturated palladium species via their CO-induced fragmentations under CO.

The structures of **3** and **4** have already been reported.[5b,3e] We emphasize here only the variations in the spatial positions of the Au atoms in structures **3** and **4**. In Figure 2a, which displays the cubic close-packed (ccp) ν_2-octahedral Au-centered Au_2Pd_{17} kernel of Au_2Pd_{21} **3**,[5b] the two Au atoms within the

dx.doi.org/10.1021/ic502470m | Inorg. Chem. 2015, 54, 1145–1151

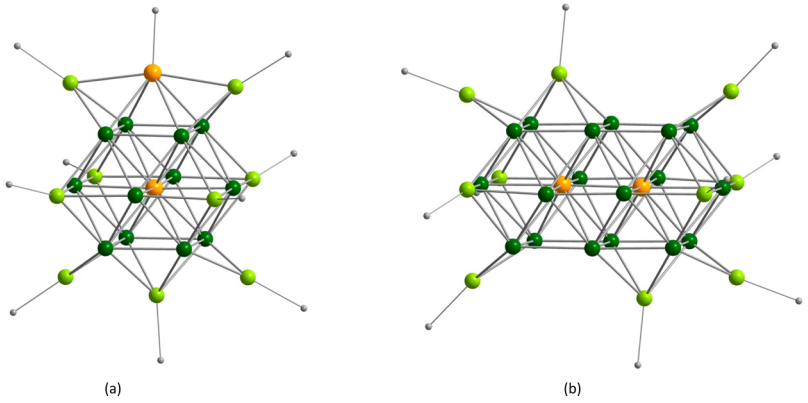

Figure 2. Molecular geometries of neutral Au_2−Pd nanoclusters **3** and **4** (without CO ligation): (a) $Au_2Pd_{21}P_{10}$ fragment of *pseudo*-C_{2v} (2 mm) **3**[5b] (without P-attached Et substituents). Its Au_2Pd_{21} core consists of a 13-atom Au(i)-interior cuboctahedral $AuPd_{12}$ kernel [Au in yellow; Pd(cub) in dark green] that is capped on its six Pd_4 faces by the other PEt_3-ligated Au(ap) and five PEt_3-ligated Pd [viz., 1Au(ap) in yellow and 1Pd(ap); 4Pd(eq) in light green] and additionally edge-bridged by four PEt_3-ligated wingtip (exopolyhedral) Pd(exo) (in light green). Two Pd(exo) are weakly connected to Au(ap). (b) $Au_2Pd_{28}P_{10}$ fragment of *pseudo*-C_{2h} (2/*m*) **4**[3e] (without P-attached Et substituents). Its Au_2Pd_{28} core consists of a 20-atom Au_2-interior bicuboctahedral Au_2Pd_{18} kernel [Au in yellow; Pd(cub) in dark green] that is capped on six of its eight Pd_4 faces by six PEt_3-ligated Pd [viz., four Pd(eq); two Pd(ap) in light green] and additionally edge-bridged by four PEt_3-ligated wingtip (exopolyhedral) Pd(exo) (in light green).

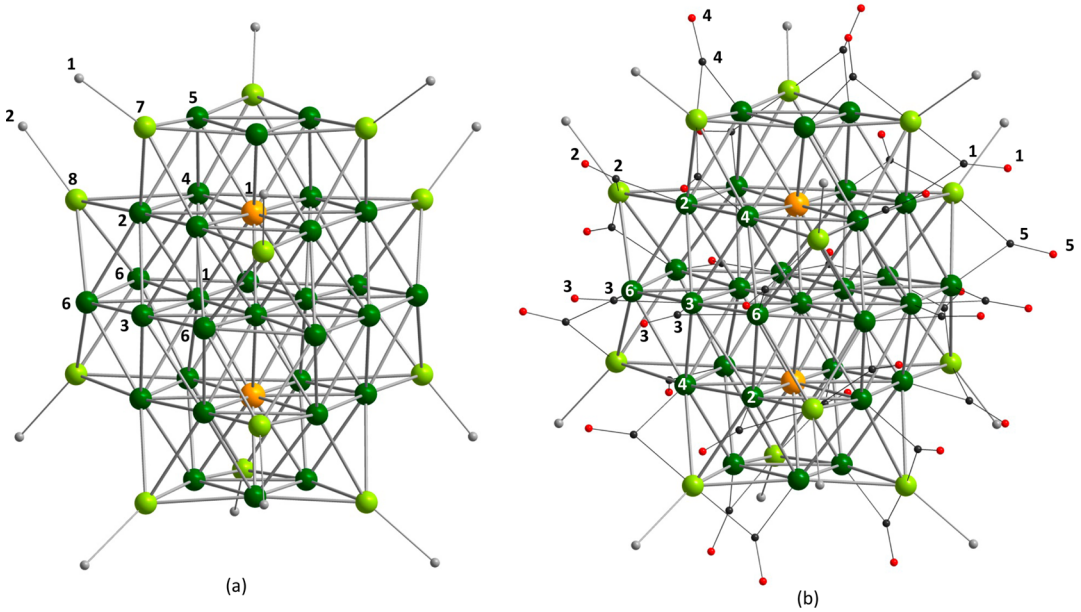

Figure 3. Structure of the five-layer hcp **1** (without P-attached Et substituents): (a) $Au_2Pd_{42}P_{12}$ fragment with a parallel **a**/**b**/**a**/**b**/**a** = Pd_6/$AuPd_9$/Pd_{12}/$AuPd_9$/Pd_6 layer sequence of *pseudo* D_{3h} symmetry. (b) $Au_2Pd_{42}(CO)_{30}P_{12}$ fragment including five independent carbonyl ligands under crystallographic D_3 (32) symmetry. The principal vertical crystallographic C_3 axis passes through the two Au atoms and the centers of the interior equilateral Pd_3 triangles in the other three layers; each of the three equivalent horizontal C_2 axes within the middle Pd_{12} layer passes through Pd(3) and one Pd(1) of the inner $Pd(1)_3$ triangle and the midpoint of two adjacent Pd(6) atoms. The 12 PEt_3-linked Pd atoms (in light green) are each connected to one doubly bridging CO *interlayer* ligand and one doubly bridging CO *intralayer* ligand. The six *interlayer* C(1)O(1) ligands staple the two outer Pd_6/$AuPd_9$ adjacent layer pairs, while the six *interlayer* C(5)O(5) ligands staple the two inner adjacent $AuPd_9$/Pd_{12} layer pairs; the six *intralayer* C(4)O(4) ligands connect adjacent Pd atoms within the top/bottom Pd_6 layers, while the six *intralayer* C(2)O(2) ligands connect adjacent Pd atoms within the inner two $AuPd_9$ layers. Under crystallographic D_3 symmetry, the six C(3)O(3) ligands are crystal-disordered at two different bonding sites (with equal sof's of 0.5): as two "half-atom" doubly bridging *intralayer* C(3)O(3) ligands within the middle Pd_{12} layer and as two "half-atom" triply bridging *interlayer* C(3)O(3) ligands that connect two Pd atoms in the middle Pd_{12} layer with one Pd atom in an adjacent $AuPd_9$ layer (μ_3-bonding mode is not shown).

neighboring diagonal ccp $AuPd_5$ and $AuPd_6$ layers are in *nonadjacent positions*, and one of the Au atoms with an attached PEt_3 ligand lies *on the surface* of the cluster. The nonbonding distance between these two Au atoms is 4.1 Å. In contrast, in Figure 2b, which presents the hexacapped ccp interpenetrating bicuboctahedral Au_2-centered Au_2Pd_{20} kernel of Au_2Pd_{28} **4**,[3e] the two Au atoms are in *adjacent internal positions* of the two diagonal symmetry-equivalent $AuPd_6$ layers, thus giving rise to an encapsulated Au_2 *dimer* with an interior Au−Au distance of 2.81 Å. Previous DFT calculations[3e] on Au_2Pd_{28} **4** have shown that this Au−Au distance corresponds to a Wiberg bond index of 0.055 (vs 1.0 for a localized Au−Au single bond). Our hypothesis[3e] that each of the two Au $6s^1$ electrons in Au_2Pd_{28} **4** is delocalized over the entire cluster toward a Au^+ configuration

dx.doi.org/10.1021/ic502470m | *Inorg. Chem.* 2015, 54, 1145−1151

Table 1. Selected Interatomic Distances for 1 under Crystallographic D_3 Site Symmetry

connectivity	N^a	distance (Å)	connectivity	N^a	distance (Å)
		Inside of the Au_2Pd_{30} Metal Core			
Au(1)−Pd(1)	6	2.7734(8)	Pd(1)−Pd(6)	6	2.7584(13)
Au(1)−Pd(2)	6	2.8197(8)	Pd(2)−Pd(3)	6	2.8722(9)
Au(1)−Pd(4)	6	2.7870(8)	Pd(2)−Pd(4)	6, 6	2.7939(12), 2.8145(12)
Au(1)−Pd(5)	6	2.772(1)	Pd(2)−Pd(5)	6	2.7786(12)
Pd(1)−Pd(1′)	3	2.6837(18)	Pd(3)−Pd(4)	6	2.7912(9)
Pd(1)−Pd(2)	6	2.7958(9)	Pd(4)−Pd(5)	6	2.7599(11)
Pd(1)−Pd(3)	6	2.8144(11)	Pd(5)−Pd(5′)	6	2.7823(14)
Pd(1)−Pd(4)	6	2.9071(9)			
		Between Capping Pd Atoms and the Au_2Pd_{30} Metal Core			
Pd(7)−Pd(2)	6	2.9350(12)	Pd(8)−Pd(2)	6	2.7726(13)
Pd(7)−Pd(4)	6	2.8172(12)	Pd(8)−Pd(4)	6	3.0339(13)
Pd(7)−Pd(5)	6, 6	2.7211(12), 2.7787(13)	Pd(8)−Pd(6)	6, 6	2.7334(13), 2.8420(13)
		Ligands[b]			
P(1)−Pd(7)	6	2.321(4)	μ_2-C(5)O(5)−Pd(6)	6	2.056(14)
P(2)−Pd(8)[b]	6	2.305(6), 2.361(11)	μ_2-C(5)O(5)−Pd(8)	6	2.011(16)
μ_2-C(2)O(2)−Pd(2)	6	1.922(13)	μ_2-C(2)−O(2)[c]	6	1.176(17)
μ_2-C(2)O(2)−Pd(8)	6	2.037(15)	μ_2-C(4)−O(4)[c]	6	1.159(16)
μ_2-C(4)O(4)−Pd(5)	6	1.918(14)	μ_2-C(5)−O(5)[c]	6	1.141(18)
μ_2-C(4)O(4)−Pd(7)	6	2.074(14)			

[a] N denotes the number of symmetry-equivalent connectivities. [b] P(2) is crystal-disordered over two sites with a sof of 0.68/0.32. [c] Distances are given for three nondisordered CO groups; the doubly bridging C(1)O(1) ligand linking the Pd_6 and $AuPd_9$ layers is crystal-disordered over two sites with a sof of 0.58/0.42; the C(3)O(3) ligand is crystal-disordered over doubly and triply bridging positions (as described in Figure 3b).

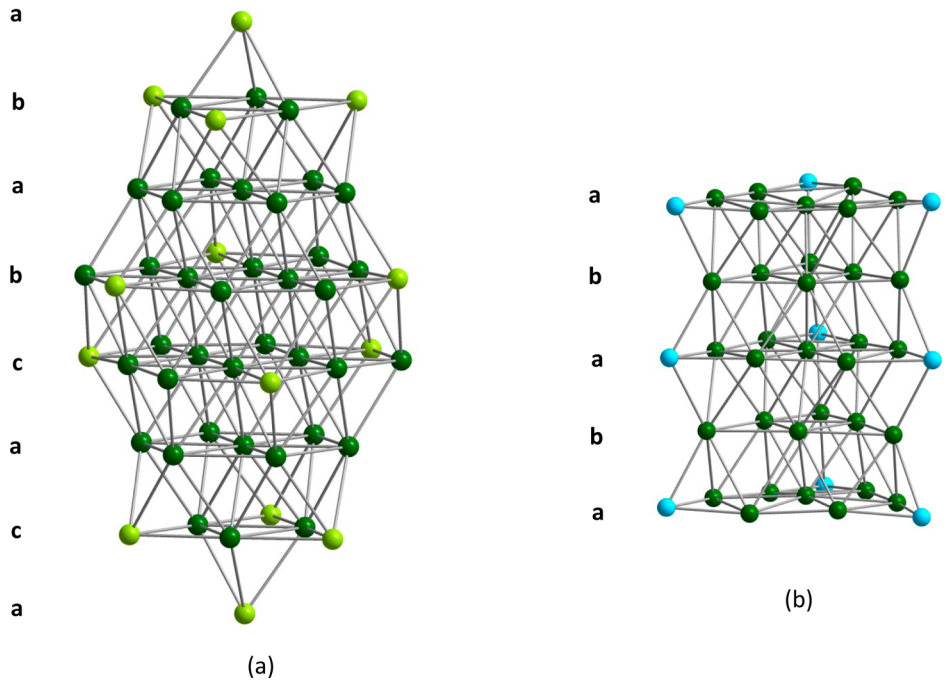

Figure 4. Metal cores of two geometrically related stacked layered structures: (a) ccp/hcp $Pd_{52}(CO)_{36}(PEt_3)_{14}$;[2b] (b) hcp $[Ni_9Pd_{33}(CO)_{41}(PPh_3)_6]^{4-}$ (as the $[PPh_4]^+$ salt).[10] PEt_3-ligated Pd atoms are in light green, Ni atoms in blue, and all other Pd atoms in dark green.

was experimentally based upon the observed *increase* by 0.04 Å in the Au−Au distance relative to that of 2.77 Å for the corresponding interior Pd−Pd distance in the isostructural Pd_{30} cluster, $Pd_{30}(CO)_{26}(PEt_3)_{10}$;[11c] the alternative formation of a *localized* electron-pair Au−Au interaction would instead give rise to a *shorter* Au−Au distance (of ∼2.60 Å).

In contradistinction to the cuboctahedral-based *ccp metal frameworks* of **3** and **4**, the molecular structure of **1** possesses the *hcp metal framework* and consists of *five layers* (namely, **a**/**b**/**a**/**b**/**a** = Pd_6/$AuPd_9$/Pd_{12}/$AuPd_9$/Pd_6) giving rise to *pseudo-*D_{3h} Au_2Pd_{42} geometry (Figure 3a). This idealized D_{3h} geometry of the $Au_2Pd_{42}P_{12}$ fragment is retained upon the addition of 12 Et_3-attached P ligands, but inclusion of 30 CO ligands (Figure 3b) reduces the *pseudo-*D_{3h} symmetry to crystallographic D_3 (32). Table 1 presents selected distances (Å) for **1** under crystallographic D_3 site symmetry. The two Au atoms, separated by the middle Pd_{12} layer, are 4.6 Å apart and are located at the apical positions of the completely encapsulated trigonal-bipyramidal $AuPd_3Au$ kernel; in turn, each Au atom centers the face-fused (μ_{12}-Au)Pd_{12} anticuboctahedra.

dx.doi.org/10.1021/ic502470m | Inorg. Chem. 2015, 54, 1145−1151

$Au_2Pd_{41}(CO)_{27}(PEt_3)_{15}$,[3f] based on three interpenetrating double icosahedra, also has a similar trigonal-bipyramidal $AuPd_3Au$ kernel, with the Au atoms being 4.7 Å apart but each centering the two highly unusual 13-vertex face-fused (μ_{13}-Au)Pd_{13} polyhedra.

The 12 PEt_3 ligands (two crystallographically independent) are coordinated to the vertex-capping Pd atoms of the outer four triangular layers (except the middle Pd_{12} one). In accordance with its solid-state structure, a $^{31}P\{^1H\}$ NMR spectrum of **1** in solution shows two singlet signals (at 18.5 and 18.0 ppm) with an intensity ratio close to 1/1. The 30 bridging COs (Figure 3b) consist of five crystallographically independent C(n)O(n) ligands (n = 1−5). With the exception of C(3)O(3), the other four independent doubly bridging C(n)O(n) ligands connect the P-bearing Pd atoms with neighboring Pd atoms of the central Au_2Pd_{30} core; the *interlayer* C(1)O(1) and C(5)O(5) staple all five layers, while C(2)O(2) and C(4)O(4) are *intralayers*. Under crystallographic D_3 site symmetry, C(3)O(3) is equally distributed over two nonequivalent positions with a site occupancy factor (sof) of 0.5: either at an *intralayer* doubly bridging position within the middle Pd_{12} layer or at one of two *interlayer* triply bridging positions that link the Pd_{12} layer with one of the two neighboring $AuPd_9$ layers; the latter *interlayer* linkage gives rise to two enantiomers based upon coordination of the C(3)O(3) ligand to either Pd(6), Pd(3), and Pd(2) or Pd(6), Pd(3), and Pd(4′); Figure 3b shows only the site-disordered doubly bridging *intralayer* linkage of C(3)O(3).

The structurally related ccp/hcp $Pd_{52}(CO)_{36}(PEt_3)_{14}$,[2b] and hcp $[Ni_9Pd_{33}(CO)_{41}(PPh_3)_6]^{4-}$ (with $[PPh_4]^+$ counterion)[10] also possess similar *parallel stacked layers* along 3-fold axes. Figure 4 displays their homometallic $Pd_{52}P_{14}$ and heterometallic $Ni_9Pd_{33}P_6$ architectures. These two clusters and **1** have an identical mean radial distance of a = 2.79 Å between the centered atoms and their 12 hcp *anti-cuboctahedral Pd* in (μ_{12}-M_{cent})Pd_{12} fragments, where M_{cent} = Pd, Au. This suggests a strain-free structural effect upon gold-for-palladium substitution in a centered position of hcp anticuboctahedra. A similar structural strain-free effect was observed upon gold-for-palladium substitution in ccp cuboctahedra in $M_2Pd_{28}(CO)_{26}(PEt_3)_{10}$, where M = Pd or Au (vide infra).[3e] The particularly noticeable difference is the *less compact* geometries of (μ_{12}-M_{cent})Pd_{12} cuboctahedra (M_{cent} = Au, Pd) in comparison with the hcp anticuboctahedral ones. Radial mean M_{cent}−Pd distances in ccp nanoclusters are as follows: $Pd_{23}(CO)_x(PEt_3)_{10}$, a = 2.85 Å [range 2.700(5)−2.914(5) Å] for x = 22,[11a] a = 2.84 Å [range 2.685(1)−2.901(1) Å] for x = 20, and a = 2.84 Å [range 2.693(1)−2.946(1) Å] for x = 21;[11b] $Pd_{30}(CO)_{26}(PEt_3)_{10}$, a = 2.84 Å [range 2.801(1)−2.877(1) Å];[11c] $Au_2Pd_{21}(CO)_{20}(PEt_3)_{10}$, a = 2.87 Å [range 2.776(2)−2.908(2) Å];[5b] $[AuPd_{22}(CO)_{20}(PPh_3)_4(PM_3)_6]^-$, a = 2.86 Å [range 2.789(4)−2.957(3) Å];[5b] $Au_2Pd_{28}(CO)_{26}(PEt_3)_{10}$, a = 2.86 Å [range 2.8070(2)−2.9395(3) Å].[3e] The radial mean distance of each centered Au atom in the above ccp Au−Pd nanoclusters is only ∼0.02 Å larger than that of the substituted zerovalent Pd atom in virtually identical ccp sites. Furthermore, the 0.02-Å-larger radial mean Au distance is consistent with the Au−Au distance of 2.811(1) Å between the two interior ccp Au atoms in Au_2Pd_{28} **4**,[3e] being 0.04 Å larger than the Pd−Pd distance of 2.773(1) Å for the corresponding two interior ccp Pd atoms in the isostructural $Pd_{30}(CO)_{26}(PEt_3)_{10}$.[11c]

The above radial mean distances in the ccp arrangements are 0.05−0.08 Å larger than those in hcp arrangements (vide supra). Because ideal ccp and hcp metal arrangements of equal-size spheres have identical space fillings (74%), this observed difference must be attributed to *ligand perturbation effects* along with crystal-packing influences. A decisive example is presented by the Pd_{52} cluster[2b] displayed in Figure 4a; in addition to its anticuboctahedral (hcp) fragment (a = 2.79 Å), it also contains a *not-less-compact* cuboctahedral (ccp) one, a = 2.78 Å. Apparently, this difference in mean distances decreases with an increase in the m/l ratio (where m denotes the total number of metal atoms and l denotes the total number of ligands). Finally, in bulk Pd (where $m/l \rightarrow \infty$), the interatomic distance reaches the ultimate "ideal" value of 2.75 Å corresponding to bulk Pd metal.[12]

CONCLUSIONS

The cationic *monogold* nanocluster **2**[5a] is found to be a versatile precursor for the preparation of three neutral *digold* Au−Pd nanoclusters under different reaction conditions: the new **1** and the known **3** and **4**. Although the driving force for each of these reactions is presumed to be similar (namely, the reduction of Au^I to Au^0), generation of the particular digold cluster is controlled by the reaction medium including the CO atmosphere. **1** and **4** were obtained from **2** under neutral or acidic conditions with appropriate CO exposure. Conversion of **2** to **3** under basic conditions occurs regardless of whether the atmosphere is CO or N_2. Under basic conditions, the initial step of these reactions likely involves nucleophilic attack of the OH^- anion on a coordinated CO ligand, whereas under neutral and acidic conditions, it likely involves CO-induced fragmentation of **2**. The three nanoclusters **1**, **3**, and **4** possess dissimilar bimetallic architectures. The hcp molecular structure of the new Au_2Pd_{42} cluster (**1**), refined under crystallographic D_3 (32) site symmetry, consists of five parallel stacked layers of $Pd_6/AuPd_9/Pd_{12}/AuPd_9/Pd_6$ that are stapled by *interlayer* CO bridging ligands. The two symmetry-equivalent Au atoms, separated by the central homopalladium Pd_{12} layer, give rise to an encapsulated $AuPd_3Au$ trigonal-bipyramidal kernel. This first isolated Au−Pd cluster with an hcp arrangement has the same *mean* radial Au−Pd anticuboctahedral distance of 2.79 Å that is found in the hcp (μ_{12}-Pd)Pd_{12} anticuboctahedral fragments of two geometrically related nanoclusters, the stacked-layer Pd_{52}[2b] and the Ni_9Pd_{33} cation ($[PPh_4]^+$ counterion);[10] these identical radial distances suggest a strain-free structural effect upon substitution of Au for Pd in their analogous hcp arrangements. It also is in accordance with our previous experimental/theoretical-based hypothesis (vide supra) for the bonding in Au_2Pd_{28} **4** being extended to **1**, such that the valence Au 6s electron of each zerovalent Au atom in Au_2Pd_{42} **1** is likewise delocalized over the entire nanocluster. Delocalization of these electrons over the palladium metal core is more favorable in **1** relative to that in **4**. In contrast to **4**, in **1** each Au atom is surrounded *entirely* by Pd atoms (less negative than Au). This, in turn, facilitates π^*-back-bonding to the CO ligands. Accordingly, the IR spectra of **1** display additional strong bands at 1828−1825 and 1800−1793 cm^{-1} (solid state) and 1780 cm^{-1} (solution) that are the lowest in the family of CO/PR_3-ligated Au−Pd clusters. This electron delocalization toward an Au^+ configuration ($6s^0$) is electronically equivalent to that of the corresponding zerovalent Pd atoms ($5s^0$) in the stacked-layer Pd_{52} and Ni_9Pd_{33} nanoclusters. Note that there is a large 0.13 Å difference between the bulk metal−metal distance in the ccp Au metal (2.884 Å) and that in the ccp Pd metal (2.751 Å) at 20 °C.[12]

dx.doi.org/10.1021/ic502470m | Inorg. Chem. 2015, 54, 1145−1151

EXPERIMENTAL SECTION

General Comments. $Au(SMe_2)Cl$, NH_4OH (ca. 30% NH_3 basis), CF_3CO_2H (99+%, *d* 1.48), and $Me_3NO{\cdot}2H_2O$ were obtained commercially. $Pd_{10}(CO)_{12}(PEt_3)_6$ was prepared analogously to $Pd_{10}(CO)_{12}(PBu^n_3)_6$[13] and recrystallized from C_6H_6/heptane. $[AuPd_{22}(CO)_{20}(PEt_3)_8][(CF_3CO_2)_2H]$ (**2**) was prepared by a published method.[5a] $^{31}P\{^1H\}$ NMR spectra were obtained under a N_2 atmosphere on a Bruker AC-300 spectrometer and referenced to 85% H_3PO_4 in D_2O as an external standard. IR spectra were recorded on a Bruker Tensor 27 Fourier transform (FT-IR) spectrometer with samples as suspensions in paratone. X-ray data for $(\mu_{12}\text{-}Au)_2Pd_{42}(CO)_{30}(PEt_3)_{12}$ (**1**) were collected at 100(2) K with a Bruker Apex 2 diffractometer (Mo Kα radiation, λ = 0.71073 Å). Analytical absorption corrections were applied (*SADABS*).[14a] The crystal structure was determined using direct methods; least-squares refinement (based on F^2) was carried out with *SHELXTL*.[14a,b] CCDC deposition number 1025553 (**1**); these data can be obtained free of charge from the Cambridge Crystallographic Data Centre via www.ccdc.cam.ac.uk/data_request/cif. See the Supporting Information.

Conversion of Cationic $[AuPd_{22}(CO)_{20}(PEt_3)_8]^+$ as $[(CF_3CO_2)_2H]^-$ Salt into $Au_2Pd_{21}(CO)_{20}(PEt_3)_{10}$ (3) under Basic Conditions. *Under a CO Atmosphere.* **2** (0.120 g, 0.028 mmol) was dissolved in a mixture of acetone/THF (4 mL/1 mL); ammonium hydroxide (0.3 mL) was added, and the atmosphere was changed from N_2 to CO. The solution was kept at room temperature for 1 day (crystals initially appeared in 1−2 h) and then at −20 °C for the following week. Black needlelike crystals of **3** (59 mg, 96%, based on Au) were washed with Me_2CO and dried under vacuum. IR spectrum (paratone) of **3**: ν(CO) 1867 (s), 1843 (w sh), 1817 (vw) cm^{-1}. $^{31}P\{^1H\}$ NMR (C_6D_6, 121 MHz): δ_1 = 26.5 (s, 1P, Au-attached), δ_2 = 4.7 (s, 4P, attached to the equatorial Pd), δ_3 = 0.7 (s, 2P, attached to two wingtip Pd that are outermost from Au), δ_4 = −0.6 (s, 1P, attached to the axial Pd), δ_5 = −3.6 (d, $^3J_{P-P}$ =5.1 Hz, 2P, attached to the wingtip Pd neighboring the axial Au) with an intensity ratio of $\delta_1/\delta_2/\delta_3/\delta_4/\delta_5$ = 0.84/4.08/2.00/1.01/2.07. Both spectra were identical with those of **3**;[5b] X-ray diffraction measurements (Mo Kα, 0.71073 Å) at 100 K of a needlelike crystal [viz., monoclinic, *a* = 26.26 Å, *b* = 15.74 Å, *c* = 27.46 Å, β = 91.13°, *V* = 11314 $Å^3$] were also identical with those of **3**.[15]

Under a N_2 Atmosphere Only. **2** (0.100 g, 0.023 mmol) was dissolved in DMF (4 mL), and NH_4OH (0.15 mL) was added; the next portion of NH_4OH (0.3 mL) was added in a few days. A total of 1 week after initiation of the reaction, 36 mg (70%, based on Au) of **3** as a black crystalline compound was isolated and identified from both spectroscopic and X-ray diffraction measurements.

Conversion of Cationic $[AuPd_{22}(CO)_{20}(PEt_3)_8]^+$ (Obtained in Situ) into $Au_2Pd_{28}(CO)_{26}(PEt_3)_{10}$ (4) under Acidic Conditions. $Pd_{10}(CO)_{12}(PEt_3)_6$ (0.100 g, 0.047 mmol) and $Me_3NO{\cdot}2H_2O$ (0.021 g, 0.189 mmol) were stirred in a mixture of acetone (4 mL) and CF_3CO_2H (0.17 mL, 2.21 mmol) under N_2 for 30 min at 50 °C; a solution of $Au(SMe_2)Cl$ (8.7 mg, 0.030 mmol) in a mixture of THF/acetone (0.7/1.3 mL) was then added dropwise followed by stirring for 2 h under N_2 at the same temperature of 50 °C. An IR spectrum of a thin film obtained via evaporation of a drop of the resulting solution was identical with that of the cationic $[AuPd_{22}(CO)_{20}(PEt_3)_8]^+$ obtained by the published procedure.[5a] The solution was cooled and filtered, and the atmosphere was changed from N_2 to CO. After 1 day, 25 mg and, after 1 week, 8 mg of additional crystals of **4** were isolated; the total yield was 42% [based on $Au(SMe_2)Cl$ as the precursor reagent]. IR spectrum (paratone) of **4**: ν(CO) 2022 (vw br), 1911 (s-m), 1884 (s), 1858 (s), 1838 (sh), 1774 (vw br) cm^{-1}. X-ray diffraction measurements (Mo Kα, 0.71073 Å) at 100 K of a block black crystal revealed a monoclinic unit cell with *a* = 19.20 Å, *b* = 17.38 Å, *c* = 19.80 Å, β = 94.84°, and *V* = 6582 $Å^3$. These crystallographic data are identical with those of **4**.[3e] Cluster **4** was also obtained under neutral conditions under CO from the preliminary isolated **2** but with a noticeably lower yield, 15−20% [also based on $Au(SMe_2)Cl$ used for the preparation of **2**]. Note that **2**, as such, has an acidic function because of its particular anion.

Conversion of Cationic $[AuPd_{22}(CO)_{20}(PEt_3)_8]^+$ as $[(CF_3CO_2)_2H]^-$ Salt into 1 under Neutral Conditions. **2** (ca. 0.14 g), obtained from $Pd_{10}(CO)_{12}(PEt_3)_6$ (0.300 g, 0.142 mmol) and $Au(SMe_2)Cl$ (26 mg, 0.088 mmol)[5a] in powder form, was kept under CO for 1 week. Its IR spectrum (paratone) was nearly the same as that of the original **2**, except for the appearance of a w-m band of a terminal CO at 2031 cm^{-1} indicative of initial decomposition. The sample was dissolved in MeCN (4.5 mL), filtered, and kept under N_2 for 1 week. A colorless solution resulted along with 20−30 mg of black crystals of **1**, ∼10−20% based on gold (with ∼80−95% contribution to a mixture of **1** and **4**), and **4** (∼5−20% in a mixture of **1** and **4**). In a modified procedure, **1** was obtained as the only crystalline product as follows. The MeCN solution was kept under N_2 for 3−6 days; the formed precipitate was filtered and extracted consecutively with Me_2CO and THF. Vapor diffusion crystallizations from both Me_2CO/i-Pr_2O and THF/hexane afforded crystals of **1** with estimated yields of 6−10 mg each. IR spectra of **1**: (paratone) ν(CO) 1875−1870 (s v br), 1838−1834 (s), 1828−1825 (s) (this band overlapped with the previous one), 1800−1793 (s) cm^{-1}; (THF) ν(CO) 1883 (s), 1843 (s), 1807 (m-w), 1780 (s) cm^{-1}. $^{31}P\{^1H\}$ NMR (C_6D_6, 121 MHz): δ_1 = 18.5 (s, 6P), δ_2 = 18.0 (s, 6P) with intensity ratio of δ_1/δ_2 = 0.90/1.00. $Au_2Pd_{42}(CO)_{30}(PEt_3)_{12}$ (**1**): $C_{102}H_{180}Au_2O_{30}P_{12}Pd_{42}$, *M* = 7120.83 g/mol; trigonal; $R\bar{3}c$; *Z* = 6; *a* = *b* = 28.2643(10) Å, *c* = 36.1195(14) Å, α = β = 90°, γ =120°; *V* = 24989.0(16) $Å^3$; *d*(calc) = 2.839 Mg/m^3; *F*(000) = 19812. Reflections (142041) obtained over 4.02° ≤ 2θ ≤ 52.00° (99.5% completeness to 2θ = 52.00°); max/min transmission coefficients, 0.5791/0.4937; μ(Mo Kα) = 6.322 mm^{-1}. Full-matrix least-squares refinement on 5437 independent merged [*R*(int) = 0.0493] reflections (276 parameters, 35 restraints) converged at wR2(F^2) = 0.1696 for all data; R1(*F*) = 0.0599 for $I > 2\sigma(I)$; GOF (on F^2) = 1.025; max/min residual electron density, 2.274 and −2.667 e/$Å^3$. Crystal size: 0.13 × 0.11 × 0.10 mm^3. The crystallographically independent unit of $Au_2Pd_{42}(CO)_{30}(PEt_3)_{12}$ (*Z* = 6), which has D_3 (32) site symmetry, consists of one Au(1) on the 3-fold axis, two Pd atoms [namely, Pd(1) and Pd(3)] on a horizontal 2-fold axis with six remaining Pd atoms as well as two PEt_3 and five CO ligands in general positions. The Et substituents of the P(1) ligand are disordered over two positions with sof's of 0.64/0.36; the second PEt_3 ligand [including the P(2) atom] is also disordered with sof's of 0.68/0.32. Two of the five independent carbonyl ligands [namely, C(1)O(1) and C(3)O(3)] are disordered over two positions with sof's of 0.58/0.42 and 0.51/0.49. All non-H atoms, except the disordered C and O atoms, were refined anisotropically. H atoms were generated geometrically. The highest residual peak Q1 with an electron density of ∼2.27 e/$Å^3$ was located at 2.8−2.9 Å from Pd(2), Pd(5), Pd(7), and Pd(8) atoms. Because these distances are typical for Pd−Pd bonding, this independent residual peak hints at the possible building of the Au_2Pd_{42} framework with six additional Pd atoms that tetracap the outer two Pd_6/$AuPd_9$ layer pairs. A similar situation was previously encountered in the two virtually identical crystal-structure determinations of the Au_2Pd_{28} cluster, where both refinements detected the existence of an additional independent Pd atom (with much greater residual densities of 10−11 e/$Å^3$) indicating the capping of unoccupied (opened) Pd_4 square faces.[3e]

ASSOCIATED CONTENT

Supporting Information

Crystallographic information file (CIF) for the structural determination of $Au_2Pd_{42}(CO)_{30}(PEt_3)_{12}$. This material is available free of charge via the Internet at http://pubs.acs.org.

AUTHOR INFORMATION

Corresponding Authors

*E-mail: mednikov@chem.wisc.edu.

*E-mail: dahl@chem.wisc.edu.

Notes

The authors declare no competing financial interest.

■ ACKNOWLEDGMENTS

This research was supported by the University of Wisconsin—Madison. The SMART 1000 CCD X-ray area-detector system was purchased, in part, with NSF Grant CHE-9310428. The Bruker AC-300 NMR spectrometer was purchased, in part, by funds from NSF Grant CHE-9208963 and NIH Grant SIO RR 08389-01. Color structural drawings were prepared with *Diamond v3.2i* (1997−2012) graphical software (Klaus Brandenburg, CrystalImpact GbR, Bonn, Germany). We thank Prof. John F. Berry (University of Wisconsin—Madison, Chemistry Department) and Prof. June L. Dahl (Department of Neuroscience; University of Wisconsin School of Medicine & Public Health) for helpful suggestions. We are also grateful to Dr. Ilia Guzei (University of Wisconsin—Madison, Chemistry Department) for use of the Departmental X-ray Crystallographic Facilities.

■ DEDICATION

Dedicated to John Corbett, an exceptionally creative and highly productive pioneer in Inorganic Chemistry for over 50 years. He was a special friend of June and Larry Dahl, who received their Ph.D. degrees in chemistry at Iowa State University during John's early career; we especially remember his warm, outgoing personality.

■ REFERENCES

(1) (a) Elschenbroich, C. *Organometallics*, 3rd ed.; VCH: Weinheim, Germany, 2006. (b) Dyson, P. J.; McIndoe, J. S. *Transition Metal Carbonyl Cluster Chemistry*; Gordon and Breach: Amsterdam, The Netherlands, 2000. (c) *Metal Clusters in Chemistry*; Braunstein, P., Oro, L. A., Raithby, P. R., Eds.; Wiley-VCH: Weinheim, Germany, 1999. (d) Longoni, G.; Iapalucci, M. C. In *Clusters and Colloids: From Theory to Applications*; Schmid, G., Ed.; VCH Publishing Inc.: New York, 1994.

(2) (a) Zacchini, S. *Eur. J. Inorg. Chem.* **2011**, 4125−4145. (b) Mednikov, E. G.; Dahl, L. F. *Philos. Trans. R. Soc. A* **2010**, *368*, 1301−1332. (c) Hogarth, G.; Kabir, S. E.; Nordlander, E. *Dalton Trans.* **2010**, *39*, 6153−6174.

(3) Aside from one-dimensional directional semistaggered oligomerization of Pt_3 triangles into $[Pt_{3n}(CO)_{6n}]^{2-}$ chains,[3i] the examples of such conversions involving metals of the Ni triad are as follows: (a) Ciabatti, I.; Femoni, C.; Gaboardi, M.; Iapalucci, M. C.; Longoni, G.; Pontiroli, D.; Ricco, M.; Zacchini, S. *Dalton Trans.* **2014**, *43*, 4388−4399 ($[H_2Co_{20}Pd_{16}C_4(CO)_{48}]^{4-}$ into $[HCo_{15}Pd_9C_3(CO)_{38}]^{2-}$ and then $[H_{3-n}Co_{15}Pd_9C_3(CO)_{38}]^{n-}$, n = 0−3, with the different Pd_9 metal cores for n = 0, 1 vs 2, 3). (b) Ciabatti, I.; de Biani, F. F.; Femoni, C.; Iapalucci, M. C.; Longoni, G.; Zacchini, S. *Dalton Trans.* **2013**, *42*, 9662−9670 ($[H_2Ni_{22}Co_6C_6(CO)_{36}]^{4-}$ into $[HNi_{36}Co_8C_8(CO)_{48}]^{5-}$). (c) Ceriotti, A.; Macchi, P.; Sironi, A.; El Afefey, S.; Daghetta, M.; Fedi, S.; de Biani, F. F.; Della Pergola, R. *Inorg. Chem.* **2013**, *52*, 1960−1964 (Pt_{19} into $Pt_{19}Au_n$, n = 3, 4). (d) Ciabatti, I.; de Biani, F. F.; Femoni, C.; Iapalucci, M. C.; Longoni, G.; Zacchini, S. *ChemPlusChem* **2013**, *78*, 1456−1465 ($[H_2Co_{20}Pd_{16}C_4(CO)_{48}]^{4-}$ into $[H_{6-n}Co_{16}Pd_2C_3(CO)_{28}]^{n-}$, n = 5, 6). (e) Mednikov, E. G.; Ivanov, S. A.; Dahl, L. F. *Inorg. Chem.* **2011**, *50*, 11795−11806 (Au_2Pd_{21} into Au_2Pd_{28}). (f) Tran, N. T.; Powell, D. R.; Dahl, L. F. *Dalton Trans.* **2004**, 217−223 (Au_2Pd_{21} into Au_2Pd_{41}). (g) Mednikov, E. G.; Ivanov, S. A.; Wittayakun, J.; Dahl, L. F. *Dalton Trans.* **2003**, 1686−1692 ($Pd_{23}P_{10}$ into $Pd_{23}P_8$ with highly dissimilar metal-core geometry). (h) Ceriotti, A.; Masciocchi, N.; Macchi, P.; Longoni, G. *Angew. Chem.* **1999**, *111*, 3941−3944; *Angew. Chem., Int. Ed.* **1999**, *38*, 3724−3727 (Pt_{19} into Pt_{38}). (i) Ciabatti, I.; Femoni, C.; Iapalucci, M. C.; Longoni, G.; Zacchini, S. *J. Cluster Sci.* **2014**, *25*, 115−146.

(4) CO/PR_3-ligated homopalladium nanoclusters were primarily obtained from $Pd_{10}(CO)_{12}(PR_3)_6$ precursors.[2b]

(5) (a) Mednikov, E. G.; Dahl, L. F. *Angew. Chem.* **2013**, *125*, 7967−7971; *Angew. Chem., Int. Ed.* **2013**, *52*, 7813−7817. (b) Tran, N. T.; Powell, D. R.; Dahl, L. F. *Dalton Trans.* **2004**, 209−216.

(6) (a) Enache, D. I.; Edwards, J. K.; Landon, P.; Solsona-Espriu, B.; Carley, A. F.; Herzing, A. A.; Watanabe, M.; Kiely, C. J.; Knight, D. W.; Hutchings, G. J. *Science* **2006**, *311*, 362−365. (b) Yang, C.-W.; Chanda, K.; Lin, P.-H.; Wang, Y.-N.; Liao, C.-W.; Huang, M. H. *J. Am. Chem. Soc.* **2011**, *133*, 19993−20000 and references cited therein. (c) Toshima, N.; Kawashima, K. *Chem. Lett.* **2012**, *41*, 1171−1172. (d) Negishi, Y. *Bull. Chem. Soc. Jpn.* **2014**, *87*, 375−389 and references cited therein. (e) Gu, X.; Lu, Z.-H.; Jiang, H.-L.; Akita, T.; Xu, Q. *J. Am. Chem. Soc.* **2011**, *133*, 11822−11825.

(7) Amiens, C.; de Caro, D.; Chaudret, B.; Bradley, J. S.; Mazel, R.; Roucau, C. *J. Am. Chem. Soc.* **1993**, *115*, 11638−11639.

(8) (a) Recently, we isolated another Au^I-containing $[(\mu_{12}\text{-Au})Pd_{22}(CO)_{20}(PEt_3)_{10}]^+$ monocation (as a $[(CF_3CO_2)_2H]^-$ salt)[8b] that is isostructural with the known homopalladium $Pd_{23}(CO)_{20}(PEt_3)_{10}$.[2b] (b) Mednikov, E. G.; Dahl, L. F. Unpublished results.

(9) The moderate reactivity of the monocation **2** toward CO is observed to be similar to that of the isostructural and *electronically equivalent* neutral homopalladium $(\mu_{14}\text{-Pd})Pd_{22}(CO)_{20}(PEt_3)_8$.[5a] In contrast, a large increase in stabilization toward a CO atmosphere occurs in homopalladium nanoclusters upon substitution of *electronically nonequivalent* zerovalent Au^0 atoms in place of zerovalent Pd^0 atoms, as exemplified by the *isostructural* **3** versus the corresponding homopalladium $Pd_{23}(CO)_{20}(PEt_3)_{10}$.[5a]

(10) Kawano, M.; Bacon, J. W.; Campana, C. F.; Dahl, L. F. *J. Am. Chem. Soc.* **1996**, *118*, 7869−7870.

(11) (a) Mednikov, E. G.; Eremenko, N. K.; Slovokhotov, Yu. L.; Struchkov, Yu. T. *J. Organomet. Chem.* **1986**, *301*, C35−C37 (Pd−Pd esd = 0.003−0.005 Å). (b) Mednikov, E. G.; Wittayakun, J.; Dahl, L. F. *J. Cluster Sci.* **2005**, *16*, 429−454. (c) Mednikov, E. G.; Ivanov, S. A.; Dahl, L. F. *Angew. Chem.* **2003**, *115*, 337−341; *Angew. Chem., Int. Ed.* **2003**, *42*, 323−327.

(12) Donohue, J. *The Structures of the Elements*; John Wiley & Sons: New York, 1974.

(13) Mednikov, E. G.; Eremenko, N. K. *Izv. Akad. Nauk SSSR. Ser. Khim.* **1982**, 2540−2545; *Bull. Acad. Sc. USSR, Div. Chem. Sc. (Engl. Transl.)* **1982**, *31*, 2240−2245.

(14) (a) *Apex2*, version 2010.7-0; Bruker-AXS Inc.: Madison, WI, 2009. (b) Sheldrick, G. M. *SHELXTL program library*, version 6.10; Bruker Analytical X-ray Systems: Madison, WI, 2000.

(15) Mednikov, E. G.; Dahl, L. F. Unpublished results.